



Phase transformation in the palladium hydrogen system: Effects of boundary conditions on phase stabilities

Alexander Dyck^a, Thomas Böhlke^a, Astrid Pundt^b, Stefan Wagner^{b,*}

^a Institute of Engineering Mechanics - Chair for Continuum Mechanics, Karlsruhe Institute of Technology (KIT), Kaiserstraße 10, 76131 Karlsruhe, Germany

^b Institute for Applied Materials – Materials Science and Engineering, Karlsruhe Institute of Technology (KIT), Engelbert-Arnold-Straße 4, 76131 Karlsruhe, Germany

ARTICLE INFO

Keywords:

Metal-hydrogen system
Thermodynamics
Mechanical stress
Phase stability
Critical temperature

ABSTRACT

Different elastic constraint conditions affect the phase stabilities of metal-hydrogen systems. This is studied considering the free energy density within a chemo-mechanically coupled approach with linear elastic deformations and homogeneous concentrations. Utilizing the palladium-hydrogen alloy as a model system, the effects of various mechanical constraints in 1D, 2D and 3D are investigated. These constraints change occurring mechanical deformations and strongly influence the systems chemical potential compared to the unconstrained system. With increasing dimensionality of the constraints, large compressive mechanical stresses occur, which destabilize the hydride phase. This yields a reduced critical temperature of hydride formation. Spinodal and equilibrium miscibility gaps of the system are deduced as a function of the boundary conditions. Notably, the critical temperature of the ideal palladium-hydrogen system with 2D constraints is predicted to be 307 K, revealing a driving force for hydride formation at room temperature even under these constraints.

As recently reported for metal-hydrogen or Li-ion battery systems, in constrained alloy systems such as thin films adhered to rigid substrates or clusters embedded in a rigid matrix, the thermodynamics of structural phase transitions is altered by the mechanical stress state [1–6]. Structural phase transitions can both be related to different crystal structures and different unit cell volumes of the phases. This results in misfit conditions at coherent interfaces, imposing high mechanical stresses [2,3,7–11]. In total, a three-dimensional stress state results, that increases the system's elastic energy density and hence changes the global chemical potential [1,12–14]. With respect to the free system, this leads to modified thermodynamic conditions of two-phase equilibria in constrained systems, unveiled in modified thermodynamic stabilities of phases, modified critical temperatures of phase transformations, as well as in shifted terminal compositions of the phases [1,9–14]. In order to study contributions of mechanical stresses, their effect on two-phase equilibria and on the coherency conditions at interfaces, metal-hydrogen systems are archetypical model systems due to the ease of their experimental handling and the well-known bulk phase diagrams [1–4,9–11,15–21]. In metal-hydrogen systems, hydrogen absorption and the formation of hydride phases result in a volume expansion of the host metal lattice scaling mainly linearly with the global hydrogen concentration [8,22,23]. In constrained systems this

lattice expansion is suppressed, depending on the actual boundary conditions. Large compressive stresses of the order of several GPa result, de-stabilizing the hydride phase [9–13,24–26]. In the present paper, we study the stability of the solid solution phase and the conditions for the onset of phase transformation applying linear elastic theory in terms of a chemo-mechanically coupled approach. The palladium-hydrogen system is utilized as model system. We aim at revealing the physical boundary conditions leading to a mechanical stress-driven suppression of the phase transformation for a given temperature. Subsequently, these effects are discussed in detail by considering the free energy and the chemical potential determining the phase stability.

Phase equilibria in hydride forming metals can be determined as minima of the free energy density ψ of the system consisting of the metal and hydrogen, according to Gibb's thermodynamics [27]. Coexisting potential troughs of the free energy density describe the thermodynamic equilibrium of the phases via the double-tangent construction [1]. In addition, in a chemo-mechanically coupled model approach, the free energy density serves as a potential for both stresses and the chemical potential [28]. Thus, in order to study metal-hydrogen systems and hydride formation, the free energy density has to be specified. In this work, the independent variables determining the free energy density are chosen to be the hydrogen concentration c in moles per volume,

* Corresponding author.

E-mail address: stefan.wagner3@kit.edu (S. Wagner).

temperature θ and occurring strains ε [28]. Commonly, the total volume specific free energy density ψ of an elastically deforming metal absorbing hydrogen is additively split in two parts [28]

$$\psi(\varepsilon, c_H) = \psi_c(c_H, \theta) + \psi_e(\varepsilon, c_H), \quad (1)$$

where the first part is chemical and depends on the temperature θ and the total dimensionless hydrogen concentration c_H in H/Pd. This dimensionless concentration is defined as the ratio between the total H-concentration c and the maximum concentration c_{\max} , thus $c_H = c/c_{\max}$. The concentration c_{\max} is the maximum hydrogen concentration achievable from a structural point of view, with $c_{\max} = 1/\nu_0$ and the volume density ν_0 of interstitial sites in moles available for hydrogen in the metal lattice. This ansatz is based on the assumption, that elastic deformations do not alter the chemical properties of the metal-hydrogen system and vice versa. The second part represents the elastic contribution due to deformations ε and chemical strains of the metal. The elastic part is a quadratic function of the elastic strains within the sample and given by [28]

$$\psi_e(\varepsilon, c_H) = \frac{1}{2} \varepsilon_e \cdot \mathbb{C} [\varepsilon_e], \quad (2)$$

where the elastic strain is the difference of the total strain and the occurring chemical strains, $\varepsilon_e = \varepsilon - \varepsilon_0$ and \mathbb{C} is the stiffness tensor of the metal. The expression $\varepsilon_e \cdot \mathbb{C} [\varepsilon_e]$ denotes the scalar product between $\mathbb{C} [\varepsilon_e]$ and ε_e , while $\mathbb{C} [\varepsilon_e]$ denotes the linear mapping of the elastic strains via the stiffness tensor. The chemical or compositional strain ε_0 results from an isotropic hydrogen-induced lattice expansion of the metal, when it occupies interstitial lattice sites being linear in the concentration [25]

$$\varepsilon_0 = \eta_H c_H \mathbf{I}, \quad (3)$$

with the lattice expansion coefficient η_H and identity tensor \mathbf{I} . The chemical part of the free energy density is given by [1,28]

$$\begin{aligned} \psi_c = & \mu_0 c_H c_{\max} + R\theta c_{\max} \left(-r \ln \left(\frac{r}{r - c_H} \right) + c_H \ln \left(\frac{c_H}{r - c_H} \right) \right) \\ & - \frac{c_{\max}}{2} E_{\text{HH}} c_H^2. \end{aligned} \quad (4)$$

Here μ_0 is a reference chemical potential, R is the gas constant and E_{HH} is a long-range attractive hydrogen-hydrogen interaction energy. It results from the interaction of dissolved hydrogen atoms via the H-induced dilatation field of the metal lattice. Hence, E_{HH} defines the driving force for the initiation of the phase transition in the metal hydrogen system [1]. The logarithmic part results from an ansatz for the mixture entropy of hydrogen with metal, with the maximum number r of hydrogen atoms per metal atom in the hydride phase. The quantity r is mainly determined by electronic interactions of H and the metal [29]. We here assume that it does not depend on the stress state of the metal. The ansatz for the entropy is equivalent to the classical mixture entropy for $r = 1$. This implies, that Eq. (4) considers both the electronic interaction of hydrogen atoms with the metal and the maximum number of interstitial sites available. As in the considered palladium – hydrogen system the electronic interaction dominates at large concentrations, the parameter r determines the maximum hydrogen concentration in Pd. From the free energy density, both the chemical potential μ_H and the mechanical stresses σ can be derived according to [28]

$$\mu_H = \frac{\partial \psi}{\partial c_H} \frac{1}{c_{\max}} = \mu_0 + R\theta \ln \left(\frac{c_H}{r - c_H} \right) - E_{\text{HH}} c_H - \eta_H \nu_0 \text{tr}(\sigma), \quad (5)$$

$$\sigma = \frac{\partial \psi}{\partial \varepsilon} = \mathbb{C} [\varepsilon - \varepsilon_e]. \quad (6)$$

Hydride formation is possible, when the chemical potential is a non-monotonous function of c_H [27]. We emphasize that this is true when no non-linear plastic deformation occurs [1]. The monotony of the chemical potential can be investigated by differentiation with respect to the

concentration and studying the sign of the resulting function. The differentiation results in

$$c_{\max} \frac{\partial^2 \psi}{\partial c_H^2} = \frac{\partial \mu_H}{\partial c_H} = \frac{R\theta r}{r c_H - c_H^2} - \nu_0 \eta_H m - E_{\text{HH}}, \quad (7)$$

where

$$m = \frac{\partial \text{tr}(\sigma)}{\partial c_H}. \quad (8)$$

Thus, for given θ and E_{HH} , the resulting stresses either suppress or allow for a phase separation, i.e., hydride formation, to occur. We note that different from this approach Alefeld [30] considered an elastic reduction of the H-H interaction strength depending on the physical boundary conditions of the system, while we distinguish the strain-induced H-H interaction and the mechanical stress impact on hydride formation. As long as there exists a spinodal composition $c_H^{\text{sp}} \in [0, r]$, for which

$$\left. \frac{\partial \mu_H}{\partial c_H} \right|_{c_H^{\text{sp}}} = 0 \quad (9)$$

holds, phase separation is possible. At the spinodal composition, any concentration fluctuation in the system builds up. Related equilibrium concentrations of the phases with the maximum solubility c_{α}^{\max} of the solid solution phase and the minimum concentration c_{β}^{\min} of the hydride phase can be deduced via Maxwell constructions of the chemical potential. Additionally, by rearranging Eq. (7), a critical temperature θ_{crit} can be determined, above which no phase separation occurs for given E_{HH} . All specified concentrations are functions of the boundary conditions. In the following, stress states for varying constraint conditions in the case of homogeneous concentrations are derived and phase separation and its suppression in the palladium-hydrogen system with different constraint conditions are studied.

Palladium is capable of interstitially absorbing hydrogen in large amounts. The volume density of available octahedral interstitial sites for hydrogen absorption is $\nu_0 = 8.94 \times 10^{-6} \text{ m}^3/\text{mol}$ and $r = 0.62 \text{ H/Pd}$ [1]. Since the parameter r is mainly determined by electronic effects [29], it is assumed here not to change with H-induced stress. Beyond the solid solution limit and below the critical temperature θ_{crit} , phase transformation with the emergence of a hydride phase can occur. At room temperature, in the Pd-H bulk system the solid solution limit of the face-centered cubic α phase is $c_{\alpha}^{\max} = 0.01 \text{ H/Pd}$, which is in equilibrium with the face-centered cubic $\beta \approx \alpha'$ phase of $c_{\alpha'}^{\max} = 0.6 \text{ H/Pd}$ composition at intermediate global H concentrations [22]. Hydrogen absorption in Pd results in an isotropic volume expansion of $\Delta V/V_0 = 0.19 c_H$ in the whole range of hydrogen concentrations [22]. Hence, the linear H-induced expansion coefficient of palladium is $\eta_H \approx 0.063$. For the palladium-hydrogen bulk system $E_{\text{HH}} = 36.8(5) \text{ kJ/mol}$ [1].

To specify the chemical potential as a function of concentration, the computation of the mechanical stresses is necessary, cf. Eq. (6). To ease the considerations and to enable comparison of the calculations with results for, e.g., Pd thin films that usually grow with [111] texture, we here consider a palladium single crystal with its [111] direction parallel to the e_z -axis of the sample coordinate system. With the elastic constants $C_{11} = 224 \text{ GPa}$, $C_{12} = 173 \text{ GPa}$ and $C_{44} = 71.6 \text{ GPa}$ of palladium, the stiffness in Voigt-Mandel notation is (for details see the supplemental material)

$$\mathbb{C} = \mathbf{Q} \star \mathbf{C}_0 \hat{=} \begin{pmatrix} 270 & 158 & 142 & -31 & 0 & 0 \\ 158 & 270 & 142 & 31 & 0 & 0 \\ 142 & 142 & 285 & 0 & 0 & 0 \\ -31 & 31 & 0 & 82 & 0 & 0 \\ 0 & 0 & 0 & 0 & 82 & -43 \\ 0 & 0 & 0 & 0 & -43 & 112 \end{pmatrix} \text{ GPa}, \quad (10)$$

where \mathbf{Q} is the rotation matrix rotating the [111] to the [001] plane, cf. the supplemental material for this publication.

Now the stress state can be specified as a linear function of the hydro-

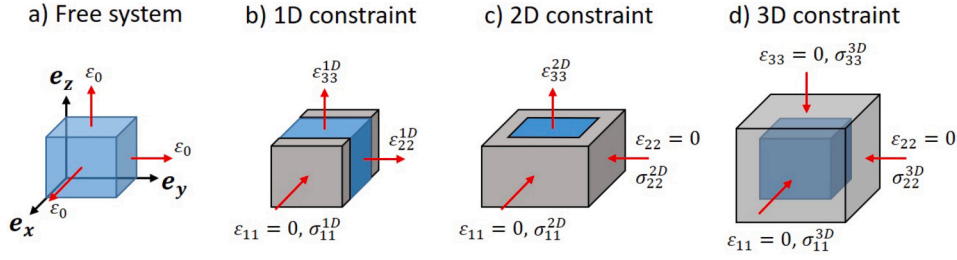


Fig. 1. Metal-hydrogen systems with different constraint conditions. Expansion of the sample cube is a) possible in all directions (0D constraint), b) suppressed in e_x -direction, c) suppressed in e_x - and e_y -direction, and d) entirely suppressed by placing the cube in a rigid shell. The gray frames visually indicate the directions of the constraint condition.

gen concentration depending on the considered constraint conditions, which are summarized in Fig. 1 for a free system (0D constraint) as well as systems with 1D, 2D and 3D constraints. We emphasize that for the 0D, 1D and 2D constrained systems stresses evolving at coherent phase interfaces are neglected. Hence, subsequently we focus on the driving force for the onset of phase transition in the homogeneous solid solution phase with the specified rigid boundary conditions. Stresses evolving at phase interfaces during phase transformation are more complex and will be targeted in a separate publication.

0D constraint For the unconstrained system of Fig. 1 a), the total strain and stress follow as

$$\epsilon^{0D} = \epsilon_0, \quad \sigma^{0D} = C [\epsilon - \epsilon_0] \hat{=} \begin{pmatrix} 0 \\ 0 \\ 0 \\ 0 \\ 0 \\ 0 \end{pmatrix} \quad (11)$$

and hence the system is stress-free.

1D constraint For the system with 1D constraint in e_x -direction in Fig. 1 b), that resembles e.g. a narrow wire that is clamped in one direction, the total strain is

$$\epsilon^{1D} \hat{=} \begin{pmatrix} 0 \\ \epsilon_{22}^{1D} \\ \epsilon_{33}^{1D} \\ 0 \\ 0 \\ 0 \end{pmatrix}, \quad (12)$$

since the system can expand freely in e_y - and in e_z -direction. Both strains follow from the stress free conditions $\sigma_{22}^{1D} = \sigma_{33}^{1D} = 0$, and the resulting stress state is

$$\sigma^{1D} = C [\epsilon^{1D} - \epsilon_0] \hat{=} \begin{pmatrix} -10 \\ 0 \\ 0 \\ 3 \\ 0 \\ 0 \end{pmatrix} c_H \text{ GPa}, \quad m^{1D} = -10 \text{ GPa}. \quad (13)$$

The non-vanishing shear stress is a result of the cubic stiffness, cf. Eq. (10), and the non-spherical total strain. However, as the chemical potential is only modified by the normal stresses, it does not influence the following discussions.

2D constraint For the 2D constrained system in Fig. 1 c), with constraints in e_x - and e_y -direction resembling e.g. a thin film with height much smaller than the lateral dimension, that adheres to a rigid substrate, the total strain is

$$\epsilon^{2D} \hat{=} \begin{pmatrix} 0 \\ 0 \\ \epsilon_{33}^{2D} \\ 0 \\ 0 \\ 0 \end{pmatrix}, \quad (14)$$

since the system can expand freely in e_z -direction. The strain ϵ_{33}^{2D} follows from the stress free condition $\sigma_{33}^{2D} = 0$, and the resulting stress state is [1]

$$\sigma^{2D} = C [\epsilon^{2D} - \epsilon_0] \hat{=} \begin{pmatrix} -18 \\ -18 \\ 0 \\ 0 \\ 0 \\ 0 \end{pmatrix} c_H \text{ GPa}, \quad m^{2D} = -36 \text{ GPa}. \quad (15)$$

3D constraint Finally, for the 3D constrained system of Fig. 1 d) resembling e.g. a cluster in a surfactant shell or rigid matrix, the total strain is

$$\epsilon^{3D} \hat{=} \begin{pmatrix} 0 \\ 0 \\ 0 \\ 0 \\ 0 \\ 0 \end{pmatrix}. \quad (16)$$

The resulting stress state, with components increasing in comparison to the 1D and 2D constraint due to Poisson's effect, is

$$\sigma^{3D} = C [\epsilon^{3D} - \epsilon_0] \hat{=} \begin{pmatrix} -36 \\ -36 \\ -36 \\ 0 \\ 0 \\ 0 \end{pmatrix} c_H \text{ GPa}, \quad m^{3D} = -108 \text{ GPa}. \quad (17)$$

The stresses of the constrained palladium-hydrogen system will strongly affect the stabilities of the solid solution phase and the hydride phase. This becomes apparent by re-writing Eq. (5) as

$$\mu_H = \mu_0 + R\theta \ln \left(\frac{c_H}{r - c_H} \right) - (\eta_H v_0 m^{XD} + E_{HH}) c_H. \quad (18)$$

Hence, the monotony of the chemical potential and thus the stability ranges of the phases in the (θ, c_H) -space will be determined by the relation of E_{HH} and the stress-dependent parameter m^{XD} . This parameter describes the stress-induced de-stabilization of the hydride phase. This is illustrated in Fig. 2 for the chemical potential of the palladium-hydrogen system with the different constraint conditions at $\theta = 300 \text{ K}$. According to Eq. (7), as long as $\partial \mu_H / \partial c_H \leq 0$, there exists a critical temperature θ_{crit} , below which the chemical potential is a non-monotonic function in increasing c_H . Then a thermodynamic driving force for the formation of the hydride phase exists. This statement is equivalent to

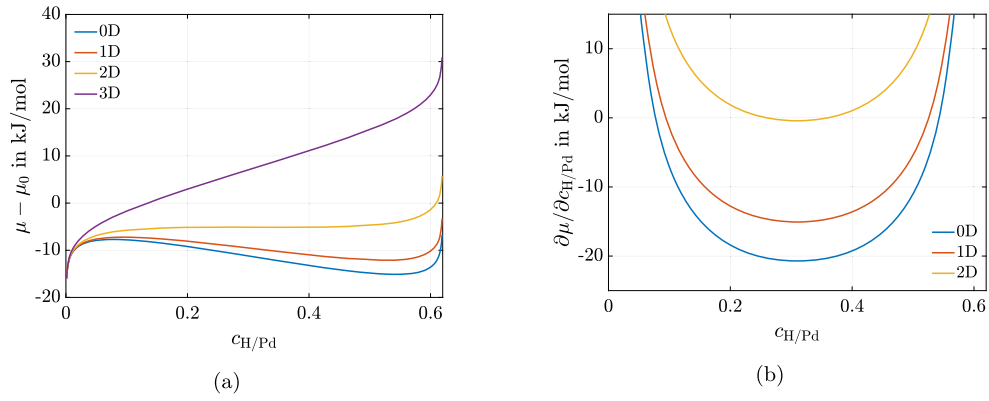


Fig. 2. a) Chemical potential of the linear-elastic palladium-hydrogen system with different constraint conditions as a function of the hydrogen concentration c_H at $\theta = 300$ K. For the free system (0D constraint) and the systems with 1D and 2D constraints, at 300 K, the chemical potential is a non-monotonous function, and hence there is a driving force for hydride formation. For 3D constraint, on the other hand, the solid solution phase is stable in the whole range of hydrogen concentrations. In detail, the overswing of the chemical potential becomes smaller with increasing constraints, revealing the stress-induced de-stabilization of the hydride phase in constrained systems. b) The derivative of the chemical potential with respect to the hydrogen concentration c_H , indicating the overswing of the chemical potential, even in the 2D constrained system.

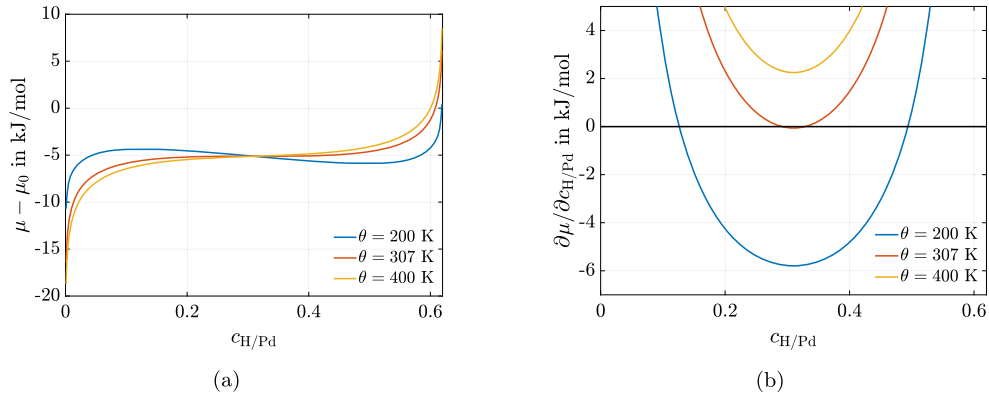


Fig. 3. a) Chemical potential of the linear elastic palladium-hydrogen system with 2D constraints, hydrogen-hydrogen interaction strength parameter $E_{HH} = 36.8$ kJ/mol and stress-contribution $\eta_H v_0 m^{2D} = -20.28$ kJ/mol in Eq. (18), plotted for different temperatures. A critical temperature $\theta_{crit} = 307$ K exists, below which the chemical potential becomes a non-convex function, yielding a thermodynamic driving force for hydride formation. b) Derivative of the chemical potential as a function of concentration. (For interpretation of the colors in the figure(s), the reader is referred to the web version of this article.)

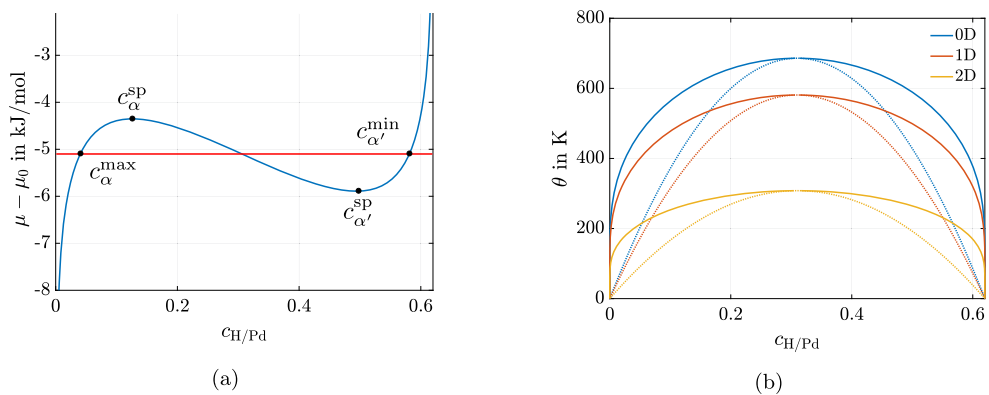


Fig. 4. a) Chemical potential as a function of the hydrogen concentration and definition of the spinodal concentrations c_{α}^{sp} and $c_{\alpha'}^{sp}$ as well as the related equilibrium concentrations c_{α}^{max} and $c_{\alpha'}^{min}$ of the phases. b) Two-phase fields of the Pd-H system for different constraint conditions. The spinodal (dotted lines) and the equilibrium (solid lines) miscibility gaps are plotted. With increasing dimensionality of the constraint conditions the miscibility gaps shrink on the temperature and the concentration axes.

the free energy density being non-convex with respect to the concentration.

For the different constraint conditions the parameters m^{XD} and the resulting critical temperatures θ_{crit} are summarized in Table 1. Apparently, up to the 2D constraint it follows $\theta_{crit} > \theta_{room}$ and, according

to Fig. 2, at room temperature even in a 2D elastically constrained palladium-hydrogen system hydride formation is predicted. This depicts the ideal condition of thin films. These results distinguish the palladium-hydrogen system from the other widely studied model system of niobium-hydrogen, where the stress-impact upon 2D constraints

Table 1

H-H interaction parameter E_{HH} initiating hydride formation, parameter m describing the stress-induced de-stabilization of the hydride phase, and resulting critical temperature θ_{crit} for the ideal palladium-hydrogen system with linear-elastic material behavior and varying constraints.

Constraint	E_{HH} in kJ/mol	m in GPa	$\eta_{\text{H}}v_0m$ in kJ/mol	θ_{crit} in K
0D	36.8	0	0	686
1D	36.8	-10	-5.63	581
2D	36.8	-36	-20.28	307
3D	36.8	-108	-60.84	no hydride formation possible

suppresses hydride formation at room temperature. This is considered in detail in a separate publication.

For the 2D constrained palladium-hydrogen system the chemical potential and its derivative with c_{H} are shown in Fig. 3 for $\theta = 200$ K, $\theta = \theta_{\text{crit}}$ and $\theta = 400$ K. Apparently, for $\theta = 200$ K (blue curve) the chemical potential is a non-convex function of hydrogen concentration, enabling two-phase equilibrium. For the critical temperature $\theta_{\text{crit}} = 307$ K, the chemical potential becomes a monotonically increasing function of c_{H} (red curve) with positive derivative, cf. Fig. 3 b).

For the palladium-hydrogen system with 3D constraints, on the contrary, evaluating Eq. (7) yields $\theta_{\text{crit}} < 0$ K and thus hydride formation is suppressed at any temperature. This resembles the result of Alefeld et al. [30], yielding the absence of phase transformation in a 3D constrained palladium-hydrogen system. We note that the calculated critical temperature of the unconstrained Pd-H system of 686 K is larger than the experimental value of 563 K [22]. This is a known issue of the theory [1], that is often regarded for by an artificial reduction of the parameter r in the classical version of Eq. (18) with $m = 0$. However, this result primarily reveals the frontiers of the models describing the thermodynamics of metal-hydrogen systems. It might be more constructive to address possible H-concentration dependencies of the elastic and the electronic interactions.

For $\theta \leq \theta_{\text{crit}}$ critical spinodal concentrations c_{H}^{sp} result, where phase transformation is feasible from a thermodynamic point of view according to Eq. (5) and Fig. 3 b). As stated above, Maxwell-constructions of the equilibrium chemical potentials for the respective conditions can then be used to determine the equilibrium concentrations of the co-existing solid-solution c_{α}^{max} and the hydride phase $c_{\alpha'}^{\text{min}}$. The spinodal and the equilibrium two-phase fields of the systems with 0D, 1D and 2D constraints are shown in Fig. 4 b). Apparently, the miscibility gap areas shrink with increasing dimensionality of the constraints.

To conclude, in this work the stability of the solid solution phase of the palladium-hydrogen system with different elastic constraint conditions and the resulting de-stabilization of the hydride phase are systematically considered within a chemo-mechanical approach. It is shown that the driving force for hydride formation decreases with progressively increasing dimensionality of the constraints. Concomitantly, the widths of the spinodal and the equilibrium two-phase coexistence regions shrink, with increasing solid solution limit, decreasing upper limit of the two-phase field and reduced critical temperature. The model predicts a driving force for hydride formation for the free system as well as for systems with 1D and 2D constraints at room temperature. For 3D constraints suppressing the H-induced volume expansion of palladium in all directions, hydride formation is entirely suppressed.

Different from the ideal linear-elastic systems stress-relaxation is often observed in constrained systems in experiments above critical hydrogen concentrations [1,2,15,16,25,31]. This can be supported by hydrogen acting as a defectant, reducing the formation energy of defects such as grain boundaries, dislocations and vacancies [32]. Stress relaxation and its impact on the systems thermodynamics will be considered in a separate publication.

CRediT authorship contribution statement

Alexander Dyck Conceptualization, Methodology, Formal analysis, Investigation, Visualization, Writing – original draft.

Thomas Böhlke: Discussion, Resources, Funding acquisition, Writing – review & editing.

Astrid Pundt: Discussion, Resources, Funding acquisition, Writing – review & editing.

Stefan Wagner: Conceptualization, Methodology, Validation, Formal analysis, Writing – original draft.

Declaration of competing interest

The authors declare that they have no known competing financial interests or personal relationships that could have appeared to influence the work reported in this paper.

Acknowledgements

AD and TB gratefully acknowledges partial funding by The Karlsruhe Institute of Technology (KIT) within the EXU funding “KIT Future Fields”, Grant ACDC.

Appendix A. Supplementary material

Supplementary material related to this article can be found online at <https://doi.org/10.1016/j.scriptamat.2024.116117>.

References

- [1] S. Wagner, A. Pundt, Quasi-thermodynamic model on hydride formation in palladium-hydrogen thin films: impact of elastic and microstructural constraints, *Int. J. Hydrog. Energy* 41 (4) (2016) 2727–2738.
- [2] S. Wagner, T. Kramer, H. Uchida, P. Dobron, J. Cizek, A. Pundt, Mechanical stress and stress release channels in 10–350 nm palladium hydrogen thin films with different micro-structures, *Acta Mater.* 114 (2016) 116–125.
- [3] R. Schwarz, A. Khachatryan, Thermodynamics of open two-phase systems with coherent interfaces, *Phys. Rev. Lett.* 74 (13) (1995) 2523.
- [4] A. Baldi, M. Gonzalez-Silveira, V. Palmisano, B. Dam, R. Griessen, Destabilization of the Mg-H system through elastic constraints, *Phys. Rev. Lett.* 102 (22) (2009) 226102.
- [5] E. Arzt, Size effects in materials due to microstructural and dimensional constraints: a comparative review, *Acta Mater.* 46 (16) (1998) 5611–5626.
- [6] M. Armand, J.-M. Tarascon, Building better batteries, *Nature* 451 (7179) (2008) 652–657.
- [7] W. Nix, B. Clemens, Crystallite coalescence: a mechanism for intrinsic tensile stresses in thin films, *J. Mater. Res.* 14 (8) (1999) 3467–3473.
- [8] J. Eshelby, The continuum theory of lattice defects, *Solid State Phys.* 3 (1956) 79–144, Elsevier.
- [9] V. Burlaka, S. Wagner, M. Hamm, A. Pundt, Suppression of phase transformation in Nb-H thin films below switchover thickness, *Nano Lett.* 16 (10) (2016) 6207–6212.
- [10] R. Griessen, N. Strohheldt, H. Giessen, Thermodynamics of the hybrid interaction of hydrogen with palladium nanoparticles, *Nat. Mater.* 15 (3) (2016) 311–317.
- [11] S. Wagner, H. Uchida, V. Burlaka, M. Vlach, M. Vlcek, F. Lukac, J. Cizek, C. Baecht, A. Bell, A. Pundt, Achieving coherent phase transition in palladium-hydrogen thin films, *Scr. Mater.* 64 (10) (2011) 978–981.
- [12] J. Weissmuller, C. Lemier, On the size dependence of the critical point of nanoscale interstitial solid solutions, *Philos. Mag. Lett.* 80 (6) (2000) 411–418.
- [13] F. Larche, J.W. Cahn, The interactions of composition and stress in crystalline solids, *J. Res. Natl. Bur. Stand.* 89 (6) (1984) 467.

- [14] C. Lemier, J. Weissmüller, Grain boundary segregation, stress and stretch: effects on hydrogen absorption in nanocrystalline palladium, *Acta Mater.* 55 (4) (2007) 1241–1254.
- [15] R. Gremaud, M. Gonzalez-Silveira, Y. Pivak, S. De Man, M. Slaman, H. Schreuders, B. Dam, R. Griessen, Hydrogenography of PdHx thin films: influence of H-induced stress relaxation processes, *Acta Mater.* 57 (4) (2009) 1209–1219.
- [16] S. Wagner, A. Pundt, Mechanical stress impact on thin Pd1-xFex film thermodynamic properties, *Appl. Phys. Lett.* 92 (5) (2008).
- [17] S. Wagner, A. Pundt, Combined impact of microstructure and mechanical stress on the electrical resistivity of PdHc thin films, *Acta Mater.* 59 (5) (2011) 1862–1870.
- [18] L. Mooij, B. Dam, Hysteresis and the role of nucleation and growth in the hydrogenation of Mg nanolayers, *Phys. Chem. Chem. Phys.* 15 (8) (2013) 2782–2792.
- [19] A. Baldi, L. Mooij, V. Palmisano, H. Schreuders, G. Krishnan, B.J. Kooi, B. Dam, R. Griessen, Elastic versus alloying effects in Mg-based hydride films, *Phys. Rev. Lett.* 121 (25) (2018) 255503.
- [20] N. Patelli, M. Calizzi, L. Pasquini, Interface enthalpy-entropy competition in nanoscale metal hydrides, *Inorganics* 6 (1) (2018) 13.
- [21] Y. Manassen, H. Realpe, D. Schweke, Dynamics of H in a thin Gd film: evidence of spinodal decomposition, *J. Phys. Chem. C* 123 (18) (2019) 11933–11938.
- [22] H. Peisl, Lattice strains due to hydrogen in metals, in: *Hydrogen in Metals I: Basic Properties*, 2005, pp. 53–74.
- [23] Y. Fukai, *The Metal-Hydrogen System: Basic Bulk Properties*, vol. 21, Springer Science & Business Media, 2006.
- [24] S. Wagner, P. Klose, V. Burlaka, K. Nörthemann, M. Hamm, A. Pundt, Structural phase transitions in niobium hydrogen thin films: mechanical stress, phase equilibria and critical temperatures, *ChemPhysChem* 20 (14) (2019) 1890–1904.
- [25] K. Nörthemann, A. Pundt, Coherent-to-semi-coherent transition of precipitates in niobium-hydrogen thin films, *Phys. Rev. B* 78 (1) (2008) 014105.
- [26] J. Cahn, F. Larché, A simple model for coherent equilibrium, *Acta Metall.* 32 (11) (1984) 1915–1923.
- [27] K. Binder, Theory of first-order phase transitions, *Rep. Prog. Phys.* 50 (7) (1987) 783.
- [28] M.E. Gurtin, E. Fried, L. Anand, *The Mechanics and Thermodynamics of Continua*, Cambridge University Press, 2010.
- [29] E. Wicke, H. Brodowsky, H. Züchner, Hydrogen in palladium and palladium alloys, in: *Hydrogen in Metals II: Application-Oriented Properties*, 2005, pp. 73–155.
- [30] G. Alefeld, Phase transitions of hydrogen in metals due to elastic interaction, *Ber. Bunsenges. Phys. Chem.* 76 (8) (1972) 746–755.
- [31] Y. Pivak, H. Schreuders, M. Slaman, R. Griessen, B. Dam, Thermodynamics, stress release and hysteresis behavior in highly adhesive Pd–H films, *Int. J. Hydrog. Energy* 36 (6) (2011) 4056–4067.
- [32] R. Kirchheim, On the solute-defect interaction in the framework of a defectant concept, *Int. J. Mater. Res.* 100 (4) (2009) 483–487.